March 2003

ST-ECF Newsletter

SPACE TELESCOPE
European Coordinating Facility

This image shows one of the hollow-cathode lamps measured to characterise the emission line spectrum of the Pt/Cr-Ne source used for wavelength calibration of the Hubble spectrographs. This work forms part of the ST-ECF STIS Calibration Enhancement project and is a collaboration with the National Institute of Standards and Technology (NIST).

Florian Kerber (ST-ECF)

HST News and Status

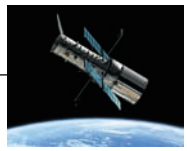

Jeremy Walsh

The tragic loss in February of the Shuttle Columbia and its crew during re-entry will probably affect the timing of the 4th major HST Servicing Mission. This mission (SM4), which will bring WFC3 to replace the almost ten year old WFPC2 and the Cosmic Origins Spectrograph (COS) to displace the COSTAR optical correction module, is currently scheduled for November 2004. Both instruments are in advanced stages of construction and the latest batch of near-infrared arrays for WFC3 may at last be of flight quality.

HST observations have been proceeding very smoothly over the past few months. The GOODS Treasury Programme of ACS imaging has successfully completed all five epochs of observation of the Chandra Deep Field South region and completed the first three epochs of Hubble Deep Field North observations. Raw data is made available immediately and release schedules for processed data, as well as further details, are available at http://www.stsci.edu/science/goods/. Plans are also well advanced for the Ultra Deep Field (UDF) which will be a single ACS pointing within the southern GOODS field, utilising 410 orbits of STScI director's discretionary time to reach significantly deeper than the original WFPC2 Hubble Deep Fields. More details about the UDF are given later in this Newsletter. Observations will probably begin in the latter half of 2003.

In early February a mysterious short circuit occurred in the HST on-board electrical power supply system. This caused considerable concern, however the problem quickly 'fixed itself'. The cause is not clear but it is suggested that a piece of space debris may have hit a Solar Panel causing the short circuit. If proven this would be the first time that a piece of debris had directly caused a problem aboard HST. Before launch there were various predictions that HST could be badly damaged by impact from a piece of 'space junk'.

The HST Cycle 12 call for proposals closed on January 24 2003. The number of proposals (1052) was very close to the number submitted in Cycle 11. The breakdown of proposals by instrument and science category shows no major differences from the last cycle, but there were more proposals in the 50-100 orbit range and fewer in the large (>100 orbit) and treasury categories. More than half of the requested orbits were for the ACS. The ESA fraction was 19%, slightly greater than in the last cycle. The HST proposal process is again setting a precedent by narrowing the interval between the Phase 1 and Phase 2 deadlines to only 3.7 months. The TAC results will be released in early April and the Phase 2 deadline is May 16.

STIS Calibration Enhancement – Spectral Characterisation of Pt/Cr-Ne Hollow Cathode Lamps

Florian Kerber, Michael R. Rosa, Craig J. Sansonetti (NIST) & Joseph Reader (NIST)**

The Instrument Physical Modelling Group at the ST-ECF is currently conducting a project aimed at improving the calibration of the Space Telescope Imaging Spectrograph (STIS) in order to increase the scientific value of the STIS archival data. This work is performed under the extension of the Memorandum of Understanding between NASA and ESA covering the Hubble Space Telescope (HST).

The STIS Calibration Enhancement (STIS-CE) concept makes heavy use of physical instrument models in place of empirical methods. A case in point is the wavelength calibration of the STIS Echelle modes for which we are going to replace the 2-D polynomial fit for the dispersion solution by a purely model-based description of the instrument's behaviour. Our post-operational archive (POA) work on the Faint Object Spectrograph (FOS) has demonstrated that this approach is robust, versatile, and more accurate than empirical methods. In the case of the FOS we have reduced the error of the dispersion solution by an order of magnitude. In order to achieve the potential of the instrument and the physical model it is imperative to have a highly accurate list of emission lines from the calibration source, hence a full characterisation of the spectral output of the STIS onboard Pt/Cr-Ne lamps. This article describes the concept and the laboratory measurements performed within the ST-ECF's Lamp Project and illustrates how the results will be used for the wavelength calibration of STIS.

Hollow Cathode Lamps in Space-based Instruments

The International Ultraviolet Explorer (IUE) became the first satellite observatory open to the astronomical community. As the satellite was intended to be used by many individual astronomers, a robust calibration procedure was required and, because of the high resolution modes available, an onboard lamp for wavelength calibration was considered mandatory. A lamp with a platinum cathode and neon fill gas was chosen based on practical considerations such as size, mass, power consumption, and lifetime, and because Pt provides a very rich emission line

* *National Institute of Standards and Technology, Gaithersburg, Maryland 20878, USA.*

Fig 1: *Original copper cathode used by Reader et al. (1990) for the first series of experiments on the Pt-Ne hollow cathode lamp. Note the silvery Pt wire in the cavity of the Cu cathode. This assembly allowed for simultaneous excitation of Pt and Cu emission, which made it possible to transfer well-established Cu II wavelength standards to the Pt spectrum.*

spectrum from 115 nm to 310 nm, the operating range of the IUE spectrograph. See Mount et al. (1977) and Fastie & Mount (1978) for details. The lamp worked reliably during the full 18 year lifetime (Jan 1978 - Sep 1996) of IUE and therefore similar lamps were selected for the first generation of spectrographs for the Hubble Space Telescope (HST) – the Goddard High Resolution Spectrograph (GHRS) (Brandt et al. 1994, Heap et al. 1995) and the Faint Object Spectrograph (FOS) (Harms et al. 1979, Harms & Fitch 1991).

For the GHRS the choice was simple. As a pure UV instrument, it had a wavelength coverage very similar to IUE. The FOS, however, had a much larger wavelength range (115 nm to 900 nm). For use in such a UV-optical instrument the Pt-Ne lamp has a major deficiency: Pt has many emission lines from 115 nm to 320 nm and Ne has strong emission from 540 nm to 800 nm. This leaves a gap in wavelength coverage of more than 200 nm. Fortunately a simple solution was found by Klose & Bridges (1987). The addition of 10% chromium to the cathode provides many more lines in the desired wavelength region, resulting in a continuous distribution of emission lines over the full wavelength range 115 nm to 900 nm. Technically, the cathode is made by mixing and sintering fine powders of Pt and Cr because the two elements do not form an alloy. In preparation for the launch of the HST the performance and operational characteristics of the hollow cathode lamps were verified in detail. In fact, because of the observed stability and predictability of the lamps in terms of radiance, Klose et al. (1990) even suggested their use as radiometric standards. Unfortunately no such work has been done on characterising the spectral output.

During the 1980s a question arose as to whether our knowledge of the spectral output of the calibration lamps would be adequate to perform a proper wavelength calibration of the high resolution modes (a few parts in 10^6) of GHRS. The Atomic Spectroscopy Group at the National Institute of Standards and Technology (NIST) in Gaithersburg, Maryland, USA, took the initiative on this issue, searching the existing literature and performing a demonstration laboratory experiment. They found that the best available wavelength values dated back to the 1930s and that their quality was not sufficient for use with the GHRS. They then conducted a full scale characterisation of the spectrum of the Pt-Ne lamp. By using a Cu cathode with a coiled up Pt wire inserted in the cavity (Figure 1) and by fine tuning the buffer gas composition and pressure, they were able to excite both Cu and Pt line emission at the same time.

As a result, they were able to transfer well-established and reliable Cu II wavelength standards to the spectrum of the Pt-Ne hollow cathode lamp. Reader at al. (1990) published a list of more than 3000 lines (110 nm to 400 nm) of Pt and Ne representing the spectrum of the Pt-Ne lamp; see their work and references therein for earlier work on the spectrum of Pt. This Pt line list has been the basis for wavelength calibration of all spectrographs onboard HST ever since – despite the fact that the FOS carried the Pt/Cr-Ne variant.

The Space Telescope Imaging Spectrograph (STIS) is a second generation HST instrument, replacing both GHRS and FOS. It was installed on the HST during the second servicing mission (STS-82) in February 1997. STIS (Woodgate et al. 1998, Kimble et al. 1998) is the first HST spectrograph to provide high resolution modes (R≈100,000) as well as large spectral coverage (115 nm to 1100 nm). Like FOS, STIS has an onboard Pt/Cr-Ne lamp for wavelength calibration. During the POA project (Rosa 2000), conducted at the ST-ECF, it was demonstrated that the Pt-Ne line list was – quite naturally – not a good match to the Pt/Cr-Ne lamp spectra of FOS. However, at the lower resolution (R≈1000) of the FOS an adequate wavelength calibration, using some unblended Pt lines only, was still achievable.

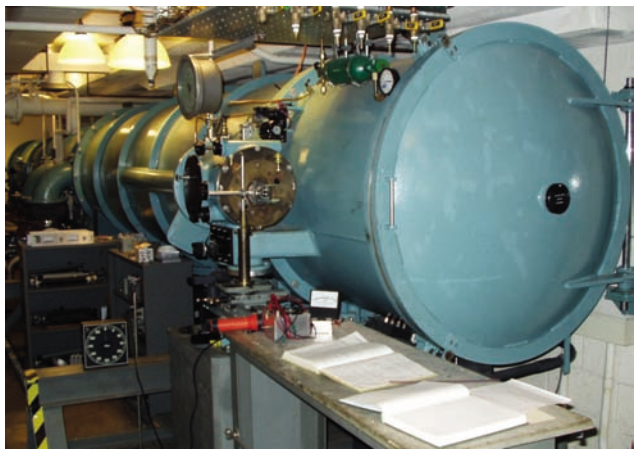

Fig 2: *The vacuum chamber of the NIST 10.7 m normal-incidence vacuum spectrograph. The hinged door at the near end provides access to the photographic plate chamber which can be isolated from the main body of the vacuum chamber.*

Fig 3: *The large roughing pump of the NIST spectrograph.*

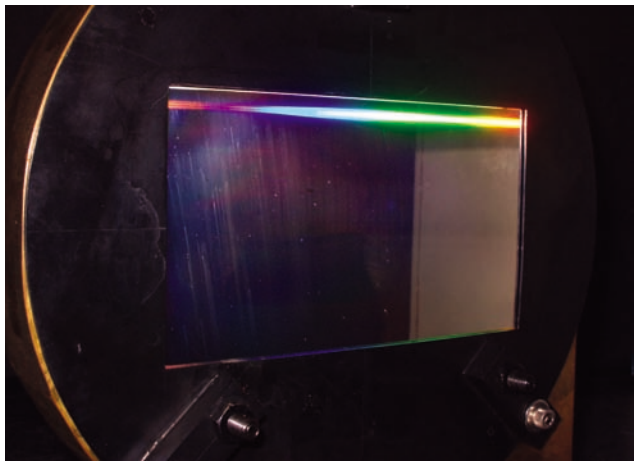

Fig 5a: *Close-up view of the concave grating.*

For the STIS-CE effort and its approach based on physical instrument models for wavelength calibration, the complete lack of information on the Cr lines is a major complication, most acutely in the Echelle modes. ESA therefore decided to fund a project to fill this gap in our understanding of the spectral output of the Pt/Cr-Ne lamp and to provide the laboratory standards that are necessary to achieve the best possible accuracy for the STIS wavelength scale. In the following we describe laboratory experiments performed in the wavelength range 115 nm to 180 nm, equivalent to the far UV (FUV) modes of STIS, and give some examples of the impact on the STIS-CE wavelength calibration.

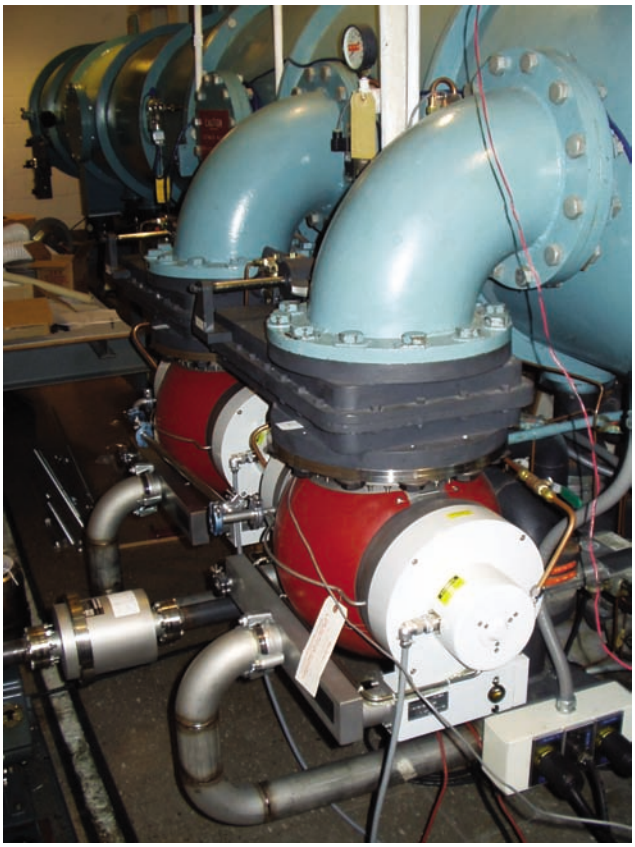

Fig 4: *The two turbo-molecular pumps attached to the vacuum vessel.*

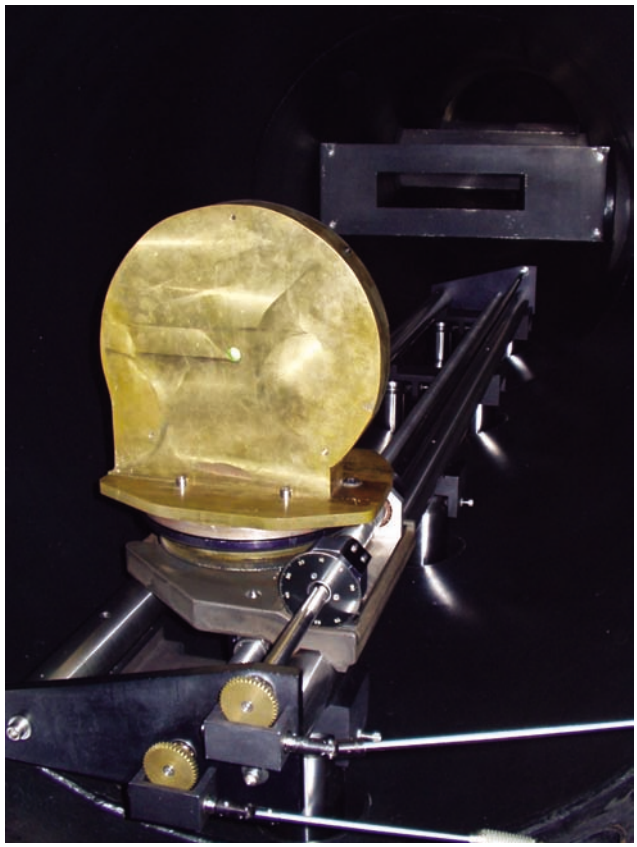

Fig 5b: *Rear view of the grating holder mounted in the spectrograph.*

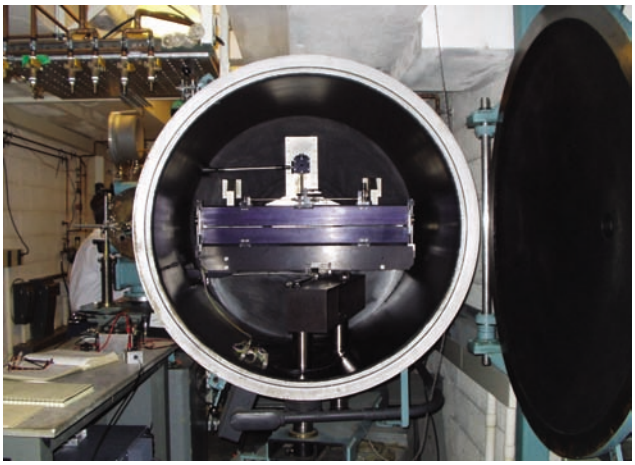

Fig 6: Open photographic plate chamber with the plate holder.

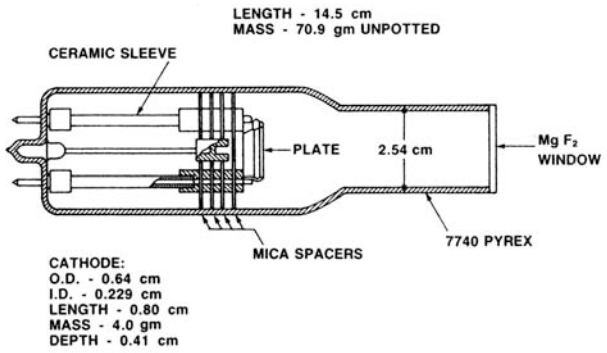

Fig 7: Schematic drawing of a hollow cathode lamp, from Klose et al. (1990).

The Experimental Set-up

The laboratory campaign for the STIS FUV modes (115 nm to 180 nm) was performed in September and October 2002. The measurements were made on the 10.7 m normal-incidence vacuum spectrograph at NIST. This Eagle mounted spectrograph is located inside a massive vacuum chamber (Figure 2). The chamber is a 13 m long cylinder with a diameter of 1.25 m at one end, tapering to 1 m at the other. The volume is about 15 m^3.

Spectra are recorded on UV sensitive photographic plates (Kodak SWR)† mounted in a plate chamber that can be isolated from the main body of the instrument. A roughing pump (Figure 3) located in a separate room can evacuate the plate chamber to a pressure of 15 Pa in about 15 min. At this pressure the plate chamber can be opened to the main body of the spectrograph which is pumped continuously by two fast turbo-molecular pumps (Figure 4).

The dispersive element for the spectrograph is a concave grating (Figure 5a and 5b) ruled with 1200 lines/mm and blazed at 120 nm. The grating is 17.5 cm wide and 10.0 cm high. In first order the spectrum is observed with a plate factor of 0.078 nm/mm and resolving power in excess of 150,000. Wavelength coverage for a single exposure is about 70 nm on two 455 mm photographic plates (Figure 6).

Hollow cathode lamps with a number of different cathode materials were used. All of the lamps were constructed with a common design shown schematically in Figure 7. Two Pt/Cr-Ne lamps, on loan from STIS Investigation Definition Team (IDT), were identical to the flight hardware. These were supplemented by newly procured Pt/Cr-Ne lamps from the same manufacturer, Imaging and Sensing Technology (IST)† of Horseheads, New York State, USA. The design of the new lamps is almost identical to the vintage flight hardware, including the special MgF_2 window assembly with the Kovar flange. Pt-Ne and Cr-Ne lamps were also observed. The lamps were operated at currents of 10 mA and 20 mA. Usually three to six spectra using different lamps or operating currents were recorded sequentially on a single pair of plates. This method greatly facilitates identification of lines from different species during the plate analysis.

Measuring the Plates

The lines on the photographic plates were measured interactively using a semi-automatic comparator (Figure 10). Each line is visually centered on an oscilloscope, and the position on the plate is registered and electronically stored. The accuracy of

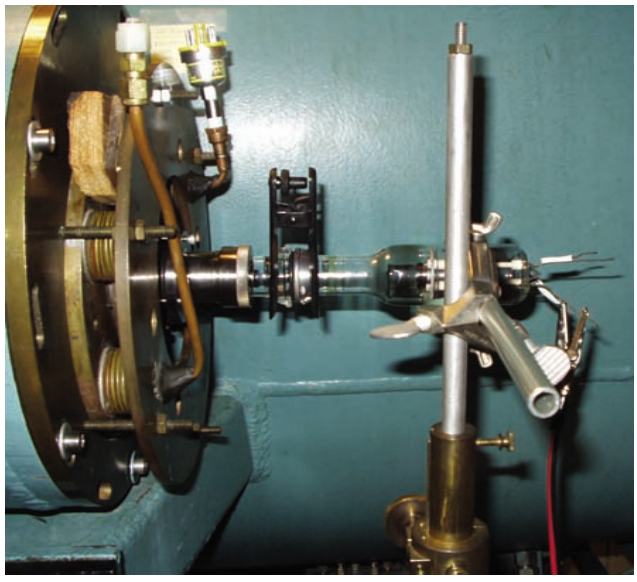

Fig 8: Lamp mounted to the spectrograph.

† *Certain commercial equipment and materials are identified in this article to adequately specify the experimental procedure. Such identification does not imply endorsement by the National Institute of Standards and Technology, nor does it imply that they are necessarily the best available for the purpose.*

Fig 9: *Sample spectra showing the visible output from the different lamps in the wavelength range 400 nm to 850 nm:*
• Pt-Ne (upper panel) has strong emission in the red part of the spectrum, only.
• Cr-Ne (middle panel) shows intense green lines.
• Pt/Cr-Ne (lower panel) has significant emission in the green while preserving a rich spectrum in the UV (not visible here).
These spectrograms were taken with a digital camera through a small spectroscope and are purely for illustration purposes.

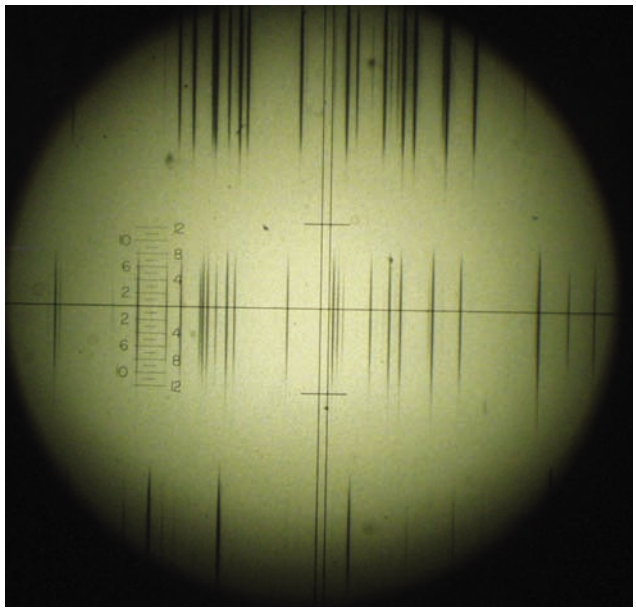

Fig 11: *Comparator display showing the spectrum around 1430 Å from three different lamps.*
• Upper spectrum: Cr-Ne
• Middle spectrum: Pt/Cr-Ne
• Lower spectrum: Pt-Ne
Only a few strong Pt lines are present in this wavelength region, whereas the Cr has a prominent series of lines here accounting for the unidentified clump in Figure 12.

the position measurement is approximately ±1µm. With the help of two identified standard lines an approximate dispersion solution is calculated and additional standard wavelengths are automatically correlated with the measured line positions. Because of the enormous focal length of the spectrograph, the dispersion is nearly linear over the entire 70 nm range. A final dispersion curve is calculated from the entire set of standard lines, typically several hundred lines of Pt I and Pt II, and used to interpolate the wavelengths of the remaining spectral lines. Figure 11 shows an example of a plate with three spectra photographed through the microscope of the comparator.

Fig 10: *The plate comparator.*

Some Results and Outlook

The measurements in the FUV range (115 nm - 185 nm) are complete and a new Pt/Cr-Ne line list has been produced. The wavelengths will be made available to the community shortly (Sansonetti et al. in preparation). Currently the line list is being used by the STIS-CE project as input for an improved wavelength calibration of STIS employing the physical instrument model. This work is in progress, and the results will be reported elsewhere.
Here we would like to present just one simple example. Figure 12 shows a long-slit spectrum of the Pt/Cr-Ne lamp from STIS ground testing. A significant number of Pt lines have been labeled by the IDT using the well-known Pt-Ne list, but the very strong and broad feature at ≈1430 Å remains unidentified. A very similar feature in FOS spectra made us aware of the lack of Cr data in the line list used by the HST calibration procedures.

This "Mystery Clump" at 1430 Å (Figure 12) was the first feature we examined during the analysis of the laboratory observations, and it was immediately evident that it consists of a number of strong Cr lines (Figure 11), which are blended at the resolution of the above STIS mode and at the resolution of the

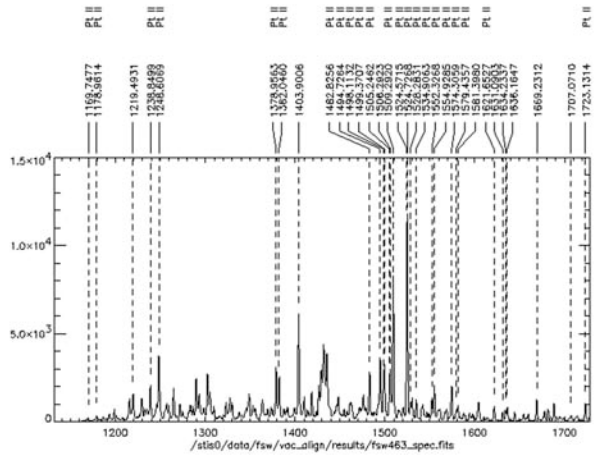

Fig 12: Pre-launch STIS spectrum of the Pt/Cr-Ne lamp.

FOS. This was the first direct confirmation of the importance of the Cr lines in the spectrum.

Detailed investigation of STIS Echelle wavelength calibration exposures in summer 2002 showed that the situation in the near UV (NUV) modes is even more severe than in the FUV with respect to the number of known lamp lines. Figure 13 shows an Echelle spectrum recorded with the NUV multi-anode multichannel array detector at a central wavelength of 2843 Å (≈80 Å total coverage). Pt lines identified with the help of the Pt-Ne list are marked by red squares. Approximately 2/3 of the lines visible on the frame remain unidentified.

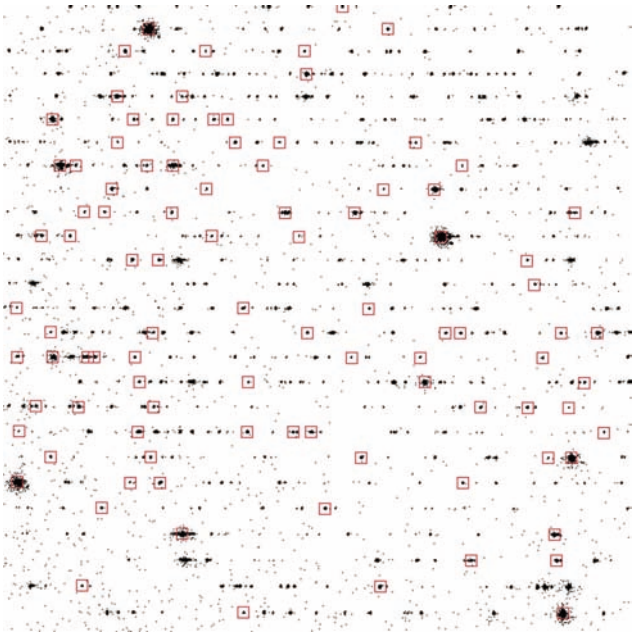

Fig 13: STIS Echelle spectrum centred at 2843 Å. Pt lines are marked with red squares. The vast majority of the unidentified lines are from Cr showing the critical need for observations in the NUV region as planned for part II of this project.

A test plate taken in the NUV region during the September laboratory campaign showed the presence of hundreds of Cr lines in this wavelength region. Part II of the lamp project is therefore dedicated to measuring the lines in the range 180 nm to 320 nm. The laboratory work using NIST's vacuum ultraviolet Fourier Transform Spectrometer (FTS) will take place during April and May, 2003. After completion of this work a comprehensive and accurate line list covering all STIS Echelle modes (115 nm to 320 nm) will be available and will form the basis of an improved wavelength calibration by the STIS-CE project.

Acknowledgements

This project benefited greatly from the involvement of Duccio Macchetto (Head of ESA's Space Telescope Operations Division) at the Space Telescope Science Institute. The help of Dan Golombek and Monica Wilson (STScI) in administrating the project is gratefully acknowledged. We thank the STIS IDT (Head: Bruce Woodgate) at Goddard Space Flight Center for providing two spare STIS lamps on loan. Special thanks go to Randy Kimble and Ted Gull (GSFC) for their logistical support.

This project is being funded by the European Space Agency (ESA). The STIS Calibration Enhancement project is conducted within the framework of the extension of the Memorandum of Understanding between NASA and ESA covering the HST.

References

• *Brandt, J.C., Heap, S.R., Beaver, E.A., et al. 1994, PASP, 106, 890*
• *Fastie, W.G., & Mount, G.H. 1978, Study of Ultraviolet Properties of Optical Components for the International Ultraviolet Explorer and for Space Telescope, NASA Contract NAS 5-23316, The Johns Hopkins University*
• *Harms, R.J., Beaver, E., Burbridge, E.M., et al. 1979, SPIE, 183, 74*
• *Harms, R., & Fitch, J. 1991, SPIE, 1494, 49*
• *Heap, S.R., Brandt, J.C., Randall, C.E., et al. 1995, PASP, 107, 871*
• *Kimble, R.A., Woodgate, B.E., Bowers, C.W., et al. 1998, ApJ, 492, L83*
• *Klose, J.Z, Hartig, G.F., & Rosenberg, W.J. 1990, Applied Optics, Vol. 29, 2951*
• *Klose, J.Z. & Bridges, J.M. 1987, Applied Optics, Vol. 26, 5202*
• *Mount, G.H., Yamasaki, G., Fowler, W., & Fastie, W.G. 1977, Applied Optics, Vol. 16, 591*
• *Reader, J. Acquista, N., Sansonetti, C.J., & Sansonetti, J.E. 1990, ApJS, 72, 831*
• *Rosa, M.R., 2000, ST-ECF Newsletter, 27, 3*
• *Sansonetti, C.J., Kerber, F., Reader, J., & Rosa, M.R. 2003, ApJS in preparation*
• *Woodgate, B.E., Kimble, R.A., Bowers, C.W., et al. 1998, PASP, 110, 1183*

An Update on Drizzle Developments

Richard Hook, Andrew Fruchter (STScI), Warren Hack (STScI) & Anton Koekemoer (STScI)

The drizzling method (Fruchter & Hook 2002) was developed long ago for the original Hubble Deep Field and has been extensively used since for the combination of dithered images. Over the last year the method has been successfully applied to images from the Advanced Camera for Surveys on Hubble where the geometric distortion is very large. This article reviews recent developments in the method and its applications. These include enhancements to the basic algorithm, wrappers to ease the application of the method to real data, both for interactive and pipeline use, and finally work in progress on making the method accessible to data analysis environments other than IRAF.

Algorithm Updates

The original drizzle method mapped a shrunken version of each input pixel onto the output and distributed weight according to the overlaps with output pixel grid. In a typical case the pixels of the output were chosen to be smaller than those of the input (the "scale" was less than one) and the "shrinking factor" (the so-called pixfrac) was around 0.5. This approach was very effective in the case of undersampled images, such as those from WFPC2, when there were multiple dithers with sub-pixel offsets. However, if the method is applied to a single image, where pixfrac and scale are both normally unity, the method becomes equivalent to bilinear interpolation. This results in an output image having strongly correlated noise and also degraded resolution. For images from the ACS in the red even the WFC channel is close to critically sampled, rather than strongly undersampled, and it would appear to be useful to consider more optimal interpolators as drizzle options. These would be implemented as new "kernels". The kernel for drizzle controls how the weight of an input pixel is distributed onto the output pixel grid. It can be thought of as equivalent to an interpolator function used in methods which sample the input image. One such optimal interpolator is the well-known "sinc" function. However, the image processing literature also contains many other such functions with many of the desirable characteristics of sinc without such heavy computational demands. One such kernel is known as "Lanczos" which may be imagined as a damped, bounded sinc. We have implemented a trial version of the Lanczos kernel in the latest version of drizzle. Figure 1 shows the gains that can follow from its application in some cases. More work is in progress to fully characterise the effect of these kernels and make recommendations for their use. This kernel will be available in the next release of the software within STSDAS.

Using the World Coordinate Systems

The basic drizzle task works in pixel space. However, most images now have a world coordinate system (WCS) in their headers which aims to provide a precise mapping from pixels to the sky. If this WCS can be relied upon (or updated to be consistent) then it provides a convenient way of specifying all the geometric information needed for drizzle to combine images. To take advantage of this there is a new version of drizzle, called wdrizzle, which is driven by the image WCS and not by user-supplied shift/rotation/scale parameters. The output is specified by a centre position (RA, Dec on the sky) along with a scale (arcsec/pixel) and an orientation (position angle of the Y-axis). This version has been widely used and tested and a public version will be made available soon.

PyDrizzle – An Intelligent Drizzle Python Wrapper

The basic drizzle task is a low-level IRAF task which requires many values from the user – the shifts, rotations, output image size etc. It is therefore not really suitable for use by itself and requires many other tasks, and not a little effort, to be used for a realistic image combination problem. To ease this process a Python script called PyDrizzle has been developed by the Science Software Branch at STScI. It provides a flexible interface, automated calculation of many parameters and integration with Pyraf – the Python-based IRAF cl replacement. It runs as a wrapper around drizzle to combine multiple images and multiple chips from the same camera.

PyDrizzle can mosaic images and rotate images to have North at the top as well as offer full control over all drizzle parameters. It makes extensive use of association tables and determines image registration parameters from the image header world-coordinate systems, with the option of small tweaks specified in the association tables.

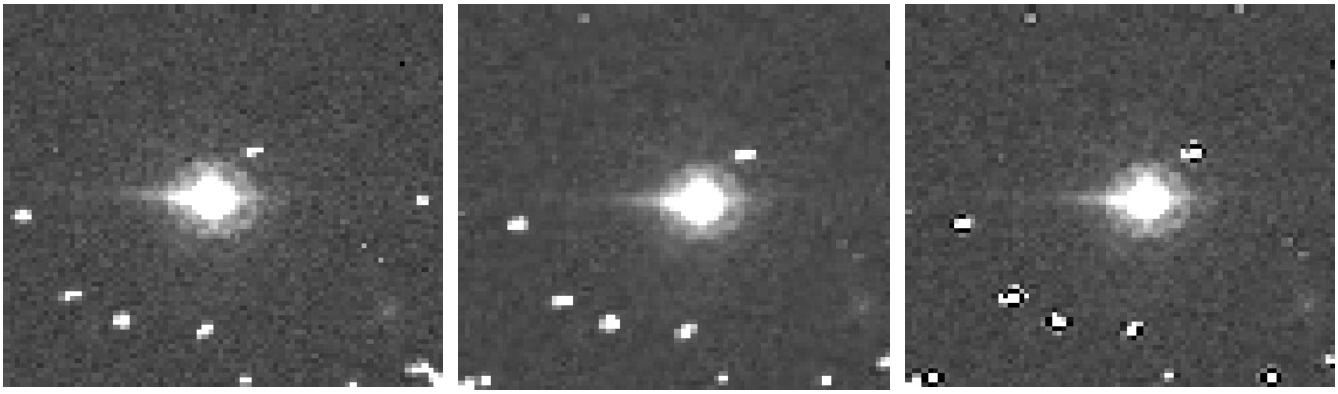

Fig 1: *Star in an ACS image through the F814W filter. Left: the original image, the FWHM of the star is 1.78 pixels. Centre: the result of drizzling the original image with kernel=square and pixfrac=1.0, the FWHM is now 2.18. Right: the result of the same drizzling with the newly implemented Lanczos kernel. The FWHM is now 1.93 pixels and there is less apparent correlated noise. Note the dark artefacts around the cosmic rays.*

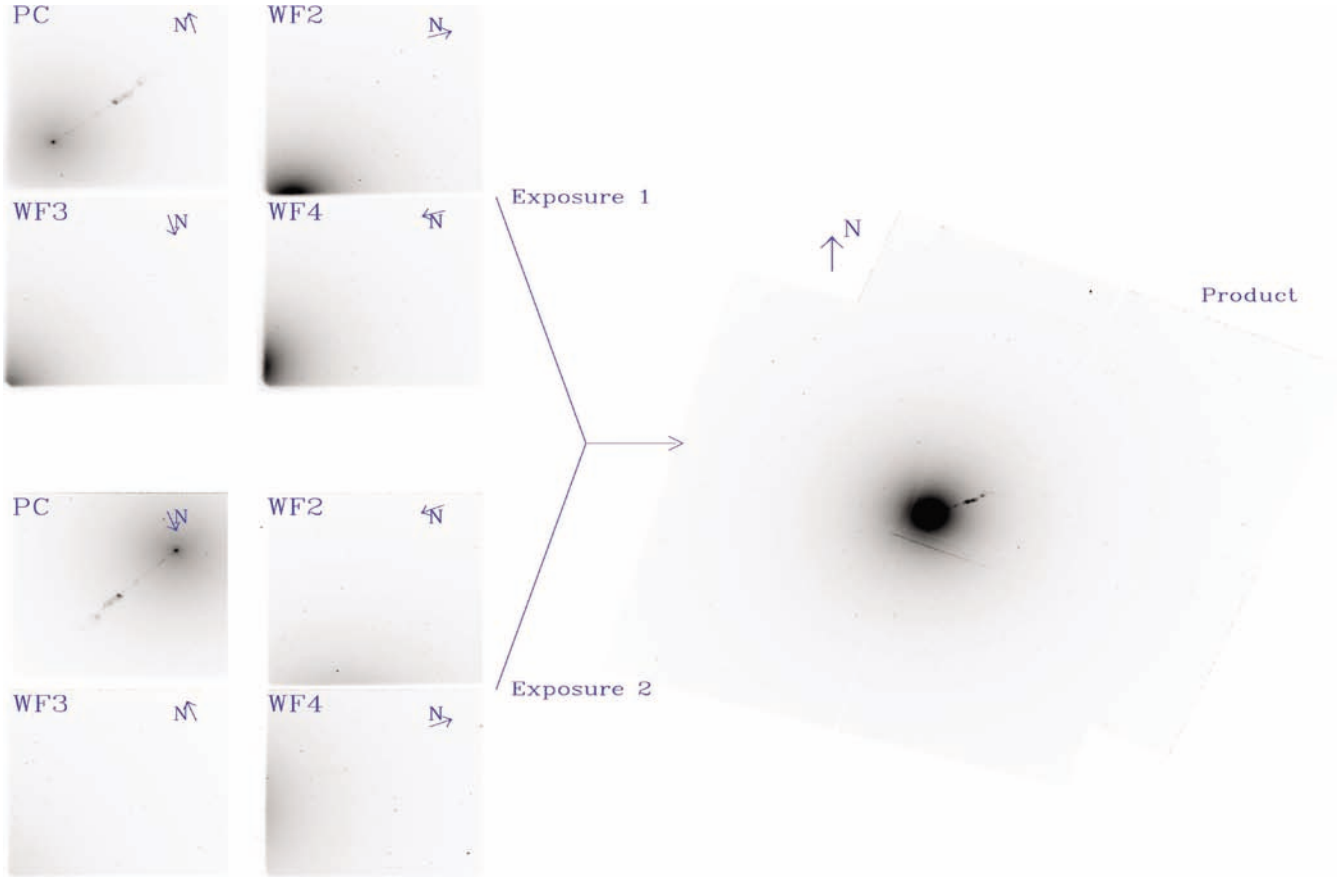

Fig 2: *PyDrizzle in action. The combination and mosaicing of WFPC2 images of M87.*

PyDrizzle is both an interactive tool, distributed as part of the STSDAS package from STScI, and also a component of the pipeline processing of ACS data at STScI. Although only currently used in the ACS pipeline PyDrizzle can be used very effectively for combining WFPC2 data (Figure 2) and is being extended for both STIS and NICMOS. PyDrizzle has an object-orientated design to ease maintenance and the addition of new features. More details are available at http://stsdas.stsci.edu/pydrizzle.

Automated Image Combination

Although PyDrizzle provides many features to automate image combination with drizzle and related tasks, it does not attack the question of combining dithered frames where there are only single frames at each dither position and hence no chance of detecting cosmic-ray hits and other artefacts by the usual CR-SPLIT mechanism. Such dithering strategies are common. A method for such generalised image combination was outlined in Fruchter and Hook (2002) and many of the tools are available in the STSDAS dither package, and more recently in PyDrizzle. A script called "metadrizzle", written in the IRAF cl, was implemented by Fruchter and Vreeswijk to automate this processing. A more recent Python-based script which solves this problem is described in the companion article on MultiDrizzle.

Callable Drizzle

A final work-in-progress which may be of interest to some is an attempt to make drizzle (and associated tasks such as blot) free of both its IRAF environment and the necessity of working to and from disk files. The aim is to make a version which can be called from another system directly, with data and parameters being passed in memory. A test version of this concept, callable from the IDL environment via the "CALL_EXTERNAL" mechanism, is working and is being used for tests of a drizzle-based version of SIRTF self-calibration. The same approach is also viable for an interface to the "numarray" Python package and such a link has been implemented and is under test.

References

Fruchter A.S. & Hook R.N., PASP, 114, 144

MultiDrizzle - Automatic Image Combination

Anton Koekemoer (STScI), Andrew Fruchter (STScI) & Warren Hack (STScI)

The idea of separating observations into multiple "dithered" exposures, each at a slightly different location, has become standard practice in HST observing as a means of mitigating the impact of hot pixels and other detector defects, as well as improving the sampling of the HST PSF, which is generally undersampled by most of the imaging instruments onboard HST. The success of these techniques in producing final cleaned images can be attributed in large part to the Drizzle software (Fruchter & Hook 2002), along with associated scripts within the IRAF/STSDAS Dither package that allow image combination and cleaning of cosmic rays. However, a major disadvantage of this suite of scripts has been its complexity, since the Dither package contains over 20 scripts, many with large numbers of parameters, and has generally required the investment of a large amount of manual effort in order to produce a final cleaned, drizzled output product.

We have therefore developed a new Python-based script, MultiDrizzle (Koekemoer et al. 2003), that is designed to provide a single-step interface to the rather complex suite of tasks that perform initial image registration, creation of a clean median image, transformation back to the input image plane, creation of cosmic ray masks, and final drizzling. The goal of MultiDrizzle is to provide a suite of user-adjustable parameters which, if left at their default values, will allow the task to perform all these steps in a single operation with no user intervention. At the same time, the parameters allow the user a large amount of power in controlling the relevant aspects of these steps, in case the default parameters are not sufficient for specific scientific applications.

In summary, MultiDrizzle can currently perform the following steps in sequence, all automatically:

- Create a mask of bad pixels, using information in the images themselves
- Carry out sky subtraction on each individual input image
- Calculate relative image shifts based on the header information
- Drizzle the input images onto a series of separate output images
- Combine these to create a clean median image
- Transform, or "blot", the median image back to the frame of the input images
- Create a cosmic ray mask based on comparing the median and its derivative with the original input image
- Perform the final drizzle combination step, applying the cosmic ray masks

Future enhancements to this script will include the ability to refine shifts based on the images themselves (by means of cataloging or cross-correlation techniques); prototypes for this already exist. Meanwhile, the script in its current form is already sufficiently robust to be exported as a beta-release to a number of HST GO teams who are now using it to combine their data. Futher details and software download are available at: http://stsdas.stsci.edu/pydrizzle/multidrizzle.

References

- *Fruchter, A. S. & Hook, R. N. 2002, PASP 114, 144*
- *Koekemoer, A. M., Fruchter, A. S., Hook, R. N., & Hack, W. 2003, in HST Calibration Workshop (STScI: Baltimore), 337*

Boomerang Nebula - the coolest place in the Universe?

The Boomerang Nebula is a young planetary nebula and the coldest object found in the Universe so far. The NASA/ESA Hubble Space Telescope image illustrates how Hubble's keen vision reveals surprises in celestial objects.

The Boomerang Nebula is one of the Universe's peculiar places. In 1995, using the 15-metre Swedish ESO Submillimetre Telescope in Chile, astronomers revealed that it is the coldest place in the Universe found so far. With a temperature of -272º C, it is only 1 degree warmer than absolute zero (the lowest limit for all temperatures). Even the -270º C background glow from the Big Bang is warmer than this nebula. It is the only object found so far that has a temperature lower than the background radiation.

The Hubble Space Telescope took this image in 1998. It shows faint arcs and ghostly filaments embedded within the diffuse gas of the nebula's smooth 'bow tie' lobes. The diffuse bow-tie shape of this nebula makes it quite different from other observed planetary nebulae, which normally have lobes that look more like 'bubbles' blown in the gas. However, the Boomerang Nebula is so young that it may not have had time to develop these structures. Why planetary nebulae have so many different shapes is still a mystery.

The general bow-tie shape of the Boomerang appears to have been created by a very fierce 500 000 kilometre-per-hour wind blowing ultracold gas away from the dying central star. The star has been losing as much as one-thousandth of a solar mass of material per year for 1500 years. This is 10-100 times more than in other similar objects. The rapid expansion of the nebula has enabled it to become the coldest known region in the Universe.

European Space Agency and NASA

Artist's impression: European Space Agency, Alfred Vidal-Madjar (Institut d'Astrophysique de Paris, CNRS, France) and NASA.

European astronomers observe first evaporating planet

Using the Hubble Space Telescope, for the first time, astronomers have observed the atmosphere of an extrasolar planet evaporating off into space. Much of this planet may eventually disappear, leaving only a dense core. The planet is a type of extrasolar planet known as a 'hot Jupiter'. These giant, gaseous planets orbit their stars very closely, drawn to them like moths to a flame.

The scorched planet called HD 209458b orbits 'only' 7 million kilometres from its yellow Sun-like star. By comparison, Jupiter, the closest gas giant in our Solar System, orbits 780 million kilometres from our Sun. The NASA/ESA Hubble Space Telescope observations reveal a hot and puffed-up evaporating hydrogen atmosphere surrounding the planet. This huge envelope of hydrogen resembles a comet with a tail trailing behind the planet. The planet circles the parent star in a tight 3.5-day orbit. Earth also has an extended atmosphere of escaping hydrogen gas, but the loss rate is much lower.

What is causing the atmosphere to escape? The planet's outer atmosphere is extended and heated so much by the nearby star that it starts to escape the planet's gravity. Hydrogen boils off in the planet's upper atmosphere under the searing heat from the star.

Perhaps the evaporation of the atmosphere plays a role in setting an inner boundary for orbits of hot Jupiters.

First Light for AVO

Markus Dolensky (ESO) on behalf of the AVO Project Team

The Astrophysical Virtual Observatory (AVO) prototype was presented at a press conference and science workshop at the Jodrell Bank radio observatory near Manchester, UK, on January 20 - 21, 2003. At this 'First Light' event the results from the first year of this three year phase A study by the six European partner organisations were presented.

Rationale

The AVO demonstration addressed some key problems of modern astronomy. These include the challenge of browsing huge sets of observations in multiple waveband regimes, where the data are distributed between several data centres. Furthermore the problem of triggering demanding remote computation on grid nodes in a way that avoids the network bottleneck was considered. The final problem was the analysis, collection and structuring of results and their visualisation.

AVO Prototype

The AVO prototype is a set of tools consisting of three software components:

1. The Aladin type of interface for metadata discovery and visualisation
2. The Astronomy Catalogue Extractor (ACE)
3. The Spectral Energy Distribution (SED) utility

The software components were developed at CDS in Strasbourg, by the Astrogrid Consortium and by ESO respectively. The three modules exchange information in VOTable format – a dialect of XML for Astronomy – and use Unified Content Descriptors (UCDs). UCDs are metadata, ie, keywords, with a defined meaning across applications and data centres. From a VO point of view UCD tagged data wrapped in VOTable format are a major innovation. Visit www.euro-vo.org/intranet/ for the details.

Fig 1: Special homemade cake to honour the AVO first light event.

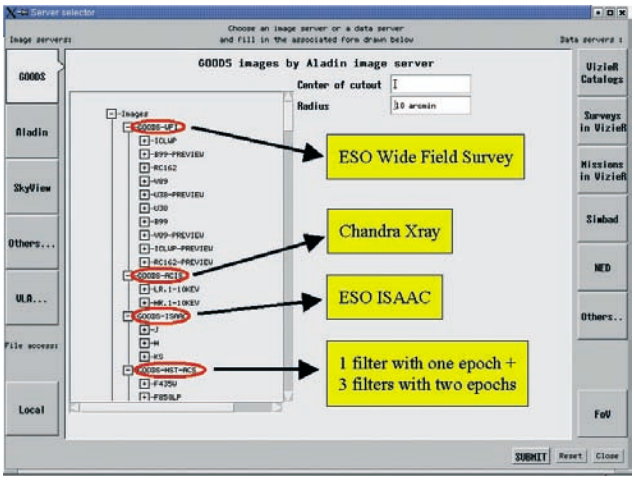

Fig 2: Hierarchical view of GOODS data in the new metadata browser.

Data

For demonstration purposes a very rich, well calibrated dataset covering many wavebands was selected from the Great Observatories Origins Deep Survey (GOODS).

Organization	Observ./Instr.	Bands
MPG/ESO	2.2m/WFI	U, B, V, R, I
ESO	VLT/ISAAC	J, H, K
NASA/ESA	HST/ACS	B, V, i, z
NASA	Chandra/ACIS	0.1 - 10 KeV
NRAO	VLA	1.4 & 8.5 GHz
UMAN/JBO	MERLIN	1.4 GHz

Tab 1: Spectral coverage including optical, infrared, X-ray and radio regime.

The ESO Imaging Survey (EIS) provided several single band as well as two cross matched colour object catalogues with 5 and 7 bands. The colour catalogues are used to generate plots of the spectral energy distribution of user selected objects. Further object catalogues from Chandra, ISO, VLA etc. help in detecting peculiar objects. Above these the Astronomy Catalogue Extractor (ACE) builds source catalogues on the fly. ACE is a web service based on the SExtractor tool. The extraction process

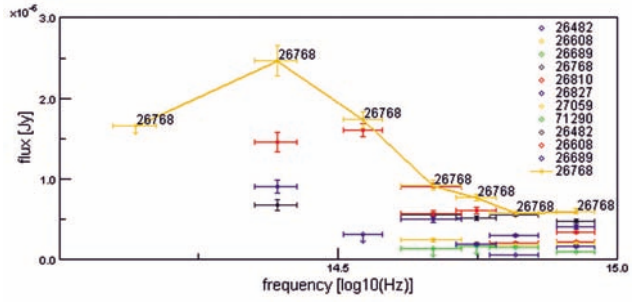

Fig 3: Spectral energy distribution of some objects in UBVRIJK bands.

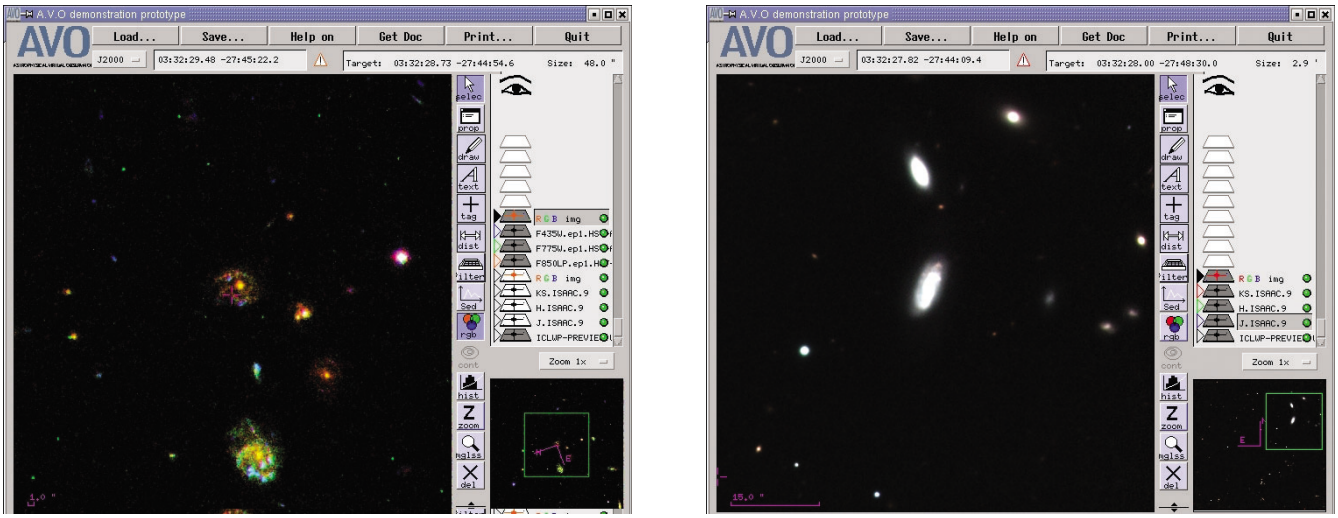

Fig 4: Analysis of the high redshift environment in 3 ACS (left) and 3 ISAAC (right) filter bands.

is configurable and the results in VOTable format can be re-imported and visualized for further analysis.

Scientific Scenarios

During the First Light event scientists presented three scenarios highlighting the potential of the AVO prototype:

1. high redshift environment
2. identification of supernova candidates
3. radio observations of Hubble Deep Field North and the associated flanking fields

All three scenarios made heavy use of the new capabilities for manipulating and analysing a hierarchical data structure comprised of image and catalogue layers together with a highly configurable filter mechanism.

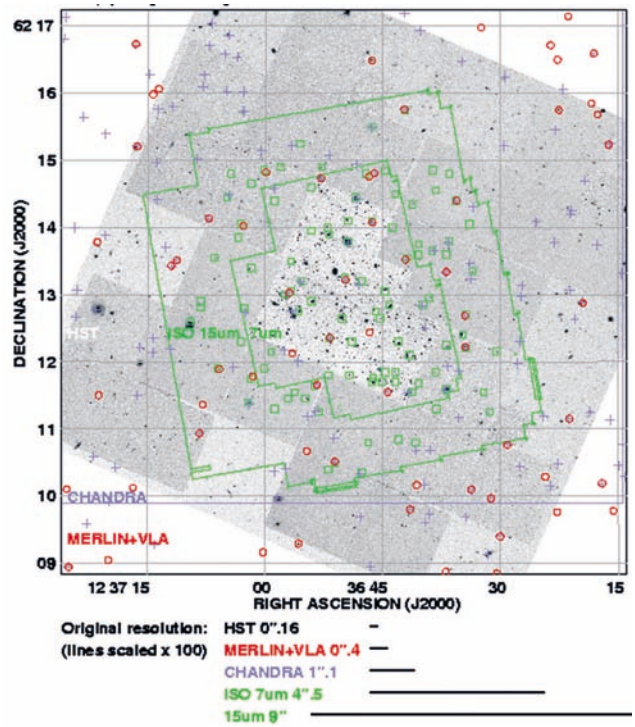

Fig 5: Fusion of HST, Chandra, Merlin and VLA data around Hubble Deep Field North

Conclusion

The AVO First Light event attracted a large number of journalists and scientists as well as representatives of the funding bodies: the European Commission and the UK Particle Physics and Astronomy Research Council (PPARC). The presentations were very well received and subsequently a number of press articles appeared. In a two-month evaluation period starting in February 2003 the AVO science working group will work out recommendations for the future. It is now a matter of defining the scope and relevant standards of a VO and ensuring that it will be attractive for data providers and scientists alike. The next science demonstration is planned for January 2004 and a third round will be in 2005. By then we will be ready for phase B – an operational Euro-VO for all observatories and astronomy data centres in Europe.

Credits

The Astrophysical Virtual Observatory was selected for funding by the 5th Framework Programme of the European Community for research, technological development and demonstration activities, contract HPRI-CT-2001-50030.

A Small Piece of GOODS and a Preview of the Hubble Ultra Deep Field

Richard Hook

This image is a 250"x250" subset of the combined BVz band Hubble/ACS data from the Great Observatories Origins Deep Survey (GOODS) ACS Treasury Programme (PI: Mauro Giavalisco at STScI). The field shown is a small part of the Chandra Deep Field South (CDF-S) and this image was built from sections of intermediate mosaics made from the first three epochs of data. The final GOODS ACS dataset, which will be made available later in the year, will cover the Hubble Deep Field North as well as CDF-S and will be the result of combining five epochs and hence significantly deeper than this preview. The total area covered by the GOODS ACS fields is around 300 square arcminutes of which this image constitutes less than 6%.

More details about GOODS, of which the ACS imaging is only one part, can be found at: http://www.stsci.edu/science/goods/.

This field will also be the location of the Hubble ACS Ultra Deep Field (UDF). This is a project initiated by the STScI Director, Steven Beckwith, to use his Director's Discretionary Time on Hubble to image a single ACS field to depths considerably beyond that achieved by the original WFPC2 Hubble Deep Fields. This survey was designed following the recommendations of a high-level Science Advisory Committee (SAC) representing most of the major space and ground observatories, and including the ESO Director General, Catherine Cesarsky. A local working group at STScI has provided detailed information to the SAC and is implementing the survey.

The UDF will use the same four filters as GOODS: F435W (B), F606W (V), F775W (i) and F850LP (z). The exposure times in the four filters will be about 55, 55, 150 and 150 orbits respectively - a total of 410 orbits. The B and V exposures are expected to reach one magnitude deeper than the equivalent HDFs and the i exposure 1.5 magnitudes deeper than the HDF F814W imaging. The z-band was not used for the original HDFs. By comparison the image shown here results from just 3 orbits in B, 1.5 in V and 3 in the z-band.

The UDF field selection followed an extensive assessment of many options. Among these were the low absorption, extensive auxiliary data sets (including the deepest Chandra imaging) and the accessibility of this field from all major ground-based observatories and, in future, from ALMA where the field will pass close to the zenith.

The exact pointing and orientation, which may change slightly in response to guide star and other implementation issues, was selected to include a z=5.8 spectroscopically confirmed galaxy as well as a spectroscopically confirmed high redshift supernova (SN 2002fw) found during the GOODS survey. Both of these objects are faintly visible on the image shown here which covers a slightly larger area than the likely UDF pointing.

The scheduling of the UDF observations is difficult, and the timing not finalised at the time of writing. Observations are likely to begin in late Summer 2003. More details of the UDF are available at: http://www.stsci.edu/science/udf.

aXe 1.2

aXe 1.2 is now available from http://www.stecf.org/software/aXe/. aXe is the ST-ECF slitless spectroscopy extraction software and was designed to facilitate the extraction and calibration of slitless spectroscopy data such as those from the ACS. The new version of aXe adds a few new features such as the possibility to assign individual weights to individual pixels in order to perform weighted extraction of faint sources. This new version is distributed with a new set of test data and a sample script. A new version of the aXe User Manual (v. 1.25) is also available. ACS Cycle 11 calibration files to use with aXe can be obtained from:
http://www.stecf.org/instruments/ACS/.

Two new CD-ROMs available

We would like to announce the availability of two new CD-ROMs from the Hubble European Space Agency Information Centre:

• The ESA/ESO Astronomy Exercise Series: This CD-ROM contains an html-structure with Adobe Acrobat PDF-files of the first six booklets in the ESA/ESO Astronomy Exercise Series. The PDF-files are available in seven languages: English, French, Italian, Spanish, Dutch, Swedish and German, as well as both high- and low-resolution versions of all the images used in the first four exercises.
• The Hubble Image Collection v.3.0: This CD-ROM contains an html-structure with both high- and low-resolution versions of some 130 of the best images taken with the NASA/ESA Hubble Space Telescope.

The CD-ROMs are free for all astronomy educators, journalists, planetaria, public observatories etc. Please e-mail to hubble@eso.org.

CONTENTS

ST-ECF

Head
Piero Benvenuti
+49-89-320 06 290
Piero.Benvenuti@stecf.org

Science Data and Software
Rudolph Albrecht
+49-89-320 06 287
Rudi.Albrecht@stecf.org

Science Instrument Information
Robert A.E. Fosbury
+49-89-320 06 235
Robert.Fosbury@stecf.org

Public Outreach
(Hubble European Space Agency Information Centre):
Lars L. Christensen
+49-89-320 06 306
lars@stecf.org

The Space Telescope-European Coordination Facility
Karl-Schwarzschild-Str.2
D-85748 Garching bei München, Germany

Website
http://www.stecf.org

Telephone
+49-89-320 06 291

Telefax
+49-89-320 06 480

Hot-line (email)
stdesk@stecf.org

Email
<user>@stecf.org

ST-ECF Newsletter

Editor
Richard Hook, Richard.Hook@stecf.org

Editorial assistant
Britt Sjöberg, Britt.Sjoeberg@stecf.org

Layout, illustrations and production
Martin Kornmesser & Lars L. Christensen

Printed by
TypeSet, München

Published by
ST-ECF